

## A SURVEY ON MULTIPLE LEVEL SET METHODS WITH APPLICATIONS FOR IDENTIFYING PIECEWISE CONSTANT FUNCTIONS

XUE-CHENG TAI AND TONY F. CHAN

(Communicated by Yanping Lin)

**Abstract.** We try to give a brief survey about using multiple level set methods for identifying piecewise constant or piecewise smooth functions. A general framework is presented. Application using this general framework for different practical problems are shown. We try to show some details in applying the general approach for applications to: image segmentation, optimal shape design, elliptic inverse coefficient identification, electrical impedance tomography and positron emission tomography. Numerical experiments are also presented for some of the problems.

**Key Words.** survey, level set methods, image segmentation, inverse problems, optimal shape design, electrical impedance tomography, positron emission tomography.

### 1. Introduction

In this work, we are trying to give a brief survey about using multiple level set methods for identifying piecewise constant or piecewise smooth functions. We try to present a general framework and then show various applications of this basic approach. The general approach presented here is originated from [12, 55, 8]. The applications we have surveyed have used this general approach or could be reformulated using this general approach for multiple level set ideas.

The general minimization problem we shall consider in this work is given in the form:

$$(1) \quad \min_{q \in K} F(q),$$

where  $K$  is a space or set containing piecewise constant functions over a given domain  $\Omega$  and possibly with some other extra constraints. Such kinds of minimization problems arise from inverse problems, optimal shape design problems, medical imaging and other applications.

In order to find a piecewise constant function, we essentially need to find the values for the constants and the location of the discontinuities. For some applications, the values of the constants are known and we only need to find the locations of the discontinuities. For two-dimensional problems, to find the locations of the discontinuities is to find the curves that separate the constant regions. For three

---

Received by the editors November 10, 2003.

2000 *Mathematics Subject Classification.* 49Q10, 49L99, 35C44, 35R30, 65J20.

We acknowledge support from the Norwegian Research Council (project numbers 135420/431), from the NSF under contracts NSF ACI-0072112, NSF INT-0072863 and NSF DMS 99-73341, from the ONR under grant N00014-96-1-10277, and from the NIH under grant P20MH65166.

dimensional problems, to find the discontinuity is to find the surface between the regions. In practical simulations, we need to use a mesh or grid. For the applications we shall consider, each constant region normally contains many mesh or grid points.

Minimization using shape derivatives have been used for finding curves and surfaces. We shall give a brief overview in Section 2 for this kind of approach. One of the potential limitations of this kind of approach is that it is difficult to handle the case that the curve or surface may disappear, merge with each other, or pinch off with each other. In this work, we shall present a different approach of using level sets to represent piecewise constant functions and embed this representation in frameworks for solving a variety of inverse problems and minimization problems with piecewise constant functions. As computational techniques, level set methods have several advantages in moving curves in 2D and surfaces in 3D. In section 3, we give an overview of the multiple level set idea first proposed in [55]. We try to supply some of the details in calculations related to gradient methods for level set ideas. It is shown that we can easily combine level set methods to calculate gradients for the considered minimization problems. Sections 4-9 are devoted to different applications. In §4, we show how to apply the level set methods for segmentation of digital images following [11, 12, 10, 9, 55]. The minimization functional is slightly different from the original Chan-Vese functional [9, 55]. In §5, we reformulate the optimal shape design problem of Osher and Santosa [42] into the framework of multiple level set methods. Applications for identifying the coefficient from an elliptic equation are presented in §6 following Chan and Tai [8]. In the original calculation of [8], augmented Lagrangian method was used to deal with the equation constraint. In §6, we show the formulation without using the augmented Lagrangian methods and some numerical tests are presented. In §7, we show applications of the level set methods for electrical impedance following Chung-Chan-Tai [18]. A similar application using level set methods for PET medical imaging is discussed in §8 following Lysaker et al [36]. In the last section §9, we show a variant of the level set methods which can be used to trace free boundary for the obstacle problems [37]. In the conclusion, we briefly mention some of the key issues in using level set methods for practical applications.

As the application of level set methods for identifying piecewise constant functions is relatively new, the works we have surveyed are mostly recent works of our research group and we must apologize for possible omissions for other recently related works.

## 2. Minimization using shape derivatives

If the constant values for a 2D piecewise constant function are known, then we just need to identify the location of the discontinuities. For such a kind of applications, the minimization problem (1) can often be transformed into the following minimization problem:

$$(2) \quad \min_{\Gamma} F(\Gamma).$$

That is, we trying to find a curve  $\Gamma$  which minimizes the functional  $F(\Gamma)$ . Traditionally, a curve is parameterized as:

$$x = x(s) \quad s \in [0, 1].$$

Correspondingly, the minimization problem (2) could be transformed into

$$(3) \quad \min_{x(s)} F(x(s)).$$

One of the common ways to find a curve which is a minimizer for (3) is to use the gradient method. First we discretize the interval  $[0, 1]$  for the space variable into  $s_0 = 0 < s_1 < s_2 < \dots < s_{N_s} = 1$ . Then we update  $x_i^n \approx x^n(s_i)$  by the formula

$$(4) \quad x_i^{n+1} = x_i^n - \alpha^n \frac{\partial F}{\partial x_i}(x^n).$$

One can also introduce an artificial time variable  $t$  and use more sophisticated methods to solve the following equation to steady state:

$$(5) \quad x_t = -\frac{\partial F}{\partial x}.$$

The weak point of such an approach is that it is hard to handle topological changes of the curves. The above procedure is sometimes referred to as particle tracing method with clear reference that the point  $x_i^n$  is used to trace the location of the point  $x_i$  at a given iteration. If the curve disappears, splits or merges during the iterations, then the iteration (4) will break down and some extra care must be taken to handle such kind of situations. In addition, there are also other difficulties related to numerical instability. For example, if the points on the curve get clustered, then the equation (5) is getting more and more stiff which will require smaller and smaller time steps to be used for the discretization of the time variables. The level set method is a good alternative for overcoming these difficulties. The level set method does not need to trace particles on the curves. Instead, a curve is represented implicitly by the zero level set of a function. By dynamically updating the level set function, the zero level set of the function is also changed. Thus, to find a curve, we just need to find the corresponding function associated with this curve. By modifying the values of a function, we can easily get the zero level curve to disappear, split or merge. We shall supply the details about the level set strategy in the next section and show applications afterwards.

### 3. Minimization using level set methods

The level set method was proposed in Osher and Sethian [43] for tracing interfaces between different phases of fluid flows. Later, it has been used for many different kind of applications involving movement of interfaces for different kind of physical problems, see [41, 48, 40, 44, 57]. In the following, we shall present a "unified" framework, first presented in [55, 8], of using multiple level sets to represent piecewise smooth functions, and use this in various problems to identify piecewise constant functions.

**3.1. An overview of level set methods.** For simplicity, let us proceed with two dimensional problems. Let  $\Gamma$  be a closed curve in  $\Omega \subset R^2$ . Associated with  $\Gamma$ , we define a  $\phi$  as a signed distance function by:

$$\phi(x) = \begin{cases} \text{distance}(x, \Gamma), & x \in \text{interior of } \Gamma \\ -\text{distance}(x, \Gamma), & x \in \text{exterior of } \Gamma. \end{cases}$$

It is clear that  $\Gamma$  is the zero level set of the function  $\phi$ . In case that  $\Gamma$  is not closed, but divide the domain into two parts, then the function can be defined to be positive on one side of the curve and negative on the other side of the curve. The function  $\phi$  is called a level set function for  $\Gamma$ . It is clear that  $\phi$  satisfies the partial differential equation:

$$(6) \quad |\nabla \phi| = 1, \quad \text{in } \Omega.$$

However,  $\phi$  is not the only function that satisfies equation (6) in the distribution sense. In order to define a unique solution for the equation, we need to introduce the

concept of viscosity solution. The existence and uniqueness of viscosity solutions for linear and nonlinear partial differential equations is an active research field with rich literature results [19]. One way to introduce the viscosity function is to add an extra time variables  $t$ . Let  $\tilde{\phi}$  be any function such that  $\Gamma$  is the zero level set curve of  $\tilde{\phi}$  and  $\tilde{\phi}$  is positive inside  $\Gamma$  and negative outside  $\Gamma$ . Then the distance function  $\phi$  is the steady state of the following time dependent equation (c.f. [41, 44, 40]):

$$(7) \quad \frac{\partial d}{\partial t} + \text{sign}(d)(|\nabla d| - 1) = 0 \quad d(x, 0) = d_0 = \tilde{\phi},$$

i.e.  $d(x, t; \tilde{\phi}) \rightarrow \phi(x)$  as  $t \rightarrow \infty$ . Moreover the steady state is unique. In applications given later, we only need the value of  $d$  in a band of width  $\epsilon$  around  $\Gamma$ . Correspondingly, we only need to solve equation (7) for  $t \leq O(\epsilon)$ .

Once the level set function is defined, we can use it to represent general piecewise constant functions. For example, assuming that  $q(x)$  equals  $c_1$  inside  $\Gamma$  and equals  $c_2$  outside  $\Gamma$ , it is easy to see that  $q$  can be represented as:

$$(8) \quad q = c_1 H(\phi) + c_2 (1 - H(\phi)),$$

where the Heaviside function  $H(\phi)$  is defined by:

$$H(\phi) = \begin{cases} 1, & \phi > 0 \\ 0, & \phi \leq 0. \end{cases}$$

In order to identify the function  $q$ , we just need to identify the level set function  $\phi$  and the piecewise constant values  $c_i$ 's.

If the function  $q(x)$  has many pieces, then we need to use multiple level set functions. We shall follow the ideas of Chan and Vese [9, 55]. Assume that we have two closed curves  $\Gamma_1$  and  $\Gamma_2$ , and we associate the two level set functions  $\phi_j, j = 1, 2$  with these curves. Then the domain  $\Omega$  is divided into four parts:

$$(9) \quad \begin{aligned} \Omega_1 &= \{x \in \Omega, \phi_1(x) > 0, \phi_2(x) > 0\}, \\ \Omega_2 &= \{x \in \Omega, \phi_1(x) > 0, \phi_2(x) < 0\}, \\ \Omega_3 &= \{x \in \Omega, \phi_1(x) < 0, \phi_2(x) > 0\}, \\ \Omega_4 &= \{x \in \Omega, \phi_1(x) < 0, \phi_2(x) < 0\}. \end{aligned}$$

Using the Heaviside function again, we can express  $q$  with possibly up to four pieces of constant values as:

$$(10) \quad q = c_1 H(\phi_1) H(\phi_2) + c_2 H(\phi_1) (1 - H(\phi_2)) + c_3 (1 - H(\phi_1)) H(\phi_2) + c_4 (1 - H(\phi_1)) (1 - H(\phi_2)).$$

By generalizing, we see that  $n$  level set functions give the possibility of  $2^n$  regions. For  $i = 1, 2, \dots, 2^n$ , let

$$\text{bin}(i - 1) = (b_1^i, b_2^i, \dots, b_n^i)$$

be the binary representation of  $i - 1$ , where  $b_j^i = 0$  or  $1$ . A piecewise constant function  $q$  with constant values  $c_i, i = 1, 2, \dots, 2^n$  could be represented as:

$$(11) \quad q = \sum_{i=1}^{2^n} c_i \prod_{j=1}^n R_i(\phi_j),$$

where

$$R_i(\phi_j) = \begin{cases} H(\phi_j), & \text{if } b_j^i = 0; \\ 1 - H(\phi_j), & \text{if } b_j^i = 1. \end{cases}$$

Even if we the true  $q$  needs less than  $2^n$  distinct regions, we can still use  $n$  level set functions since some subdomains are allowed to be empty. In using such a representation, we only need to determine the maximum number of level set functions we want to use before we start.

For some applications, the function value inside each region may not be a constant and may change slowly. For these problems, we may try to use quadratic, cubic or some higher order polynomials to approximate the function inside each region. Representations (10) and (11) can be easily generalized to higher order approximations, see [55, 14] for some details about using this idea for image problems. In this work, we shall only concentrate on applications with piecewise constant functions.

**3.2. The level set dictionary.** For every level set function  $\phi_i$ , its zero level set represents a curve  $\Gamma_i$ . It is therefore not surprising that most of the geometrical quantities of the curve  $\Gamma_i$  can be represented in term of the function  $\phi_i$ . Here, we try to recall some of the standard level set dictionary from [41, 40]. First, it is easy to see that

$$\mathbf{N} = \frac{\nabla\phi_i}{|\nabla\phi_i|}$$

is the unit normal vector of  $\Gamma_i$  pointing to the interior. The mean curvature of the curve is

$$\kappa = -\nabla \cdot \frac{\nabla\phi_i}{|\nabla\phi_i|}.$$

Moreover, we have that

$$\text{Length of } \Gamma_i = \int_{R^n} \delta(\phi_i) |\nabla\phi| dx = \int_{R^n} |\nabla H(\phi_i)| dx.$$

$$\int_{\Gamma_i} p(x) ds = \int_{R^n} p(x) \delta(\phi_i(x)) |\nabla\phi(x)| dx = \int_{R^n} p(x) |\nabla H(\phi_i(x))| dx.$$

If we denote  $\omega_i = \{x | \phi_i(x) > 0\}$ , it is easy to see that

$$\begin{aligned} \text{Area of } \omega_i &= \int_{R^n} H(\phi) dx, \\ \int_{\omega_i} p(x) dx &= \int_{R^n} p(x) H(\phi(x)) dx. \end{aligned}$$

**3.3. Combining level set methods with gradient type of methods.** Gradient type methods will be used to find the minimizers with respect to  $c_i$  and  $\phi_i$ . For minimization problem (1), assume that  $K$  is a space or set containing piecewise constant functions over a domain  $\Omega$  and possibly with some other extra constraints. For any given  $q \in K$ , it can be represented as in (11). To use gradient methods to minimize a functional  $F$  on  $K$ , we shall calculate the Gateaux differential of  $F$  [22, p.23]. The Gateaux differential shall be defined in the sense of distributions. For a given  $F : V \mapsto R$ , which maps elements from a space  $V$  to real numbers, we say that  $G(q)$  is the Gateaux differential of  $F(q)$  if

$$\lim_{\epsilon \rightarrow 0} \frac{F(q + \epsilon\mu) - F(q)}{\epsilon} = \int_{\Omega} G(q) \mu dx, \quad \forall \mu \in C_0^\infty(\Omega).$$

Normally, we write  $\partial F / \partial q = G(q)$ . Under appropriate continuity assumptions on the derivatives and related functions, the following relations are true:

$$(12) \quad \frac{\partial F}{\partial c_i} = \int_{\Omega} \frac{\partial F}{\partial q} \frac{\partial q}{\partial c_i} dx, \quad \frac{\partial F}{\partial \phi_i} = \frac{\partial F}{\partial q} \frac{\partial q}{\partial \phi_i}.$$

The above formulas are essentially the chain's rule. In the appendix, we give a brief explanation about how to get these formulas under proper continuity assumptions on  $F$  and its derivatives. For many problems, we know how to compute  $\partial F/\partial q$  and there are ready softwares to compute them. In order to use the level set method, we just need to compute the derivatives  $\partial q/\partial c_i$  and  $\partial q/\partial \phi_i$  as given later in (14) and (16).

Let us first consider a simple case where we only have one level set function and the piecewise constant function  $q(x)$  is represented as in (8). Then it is easy to see that:

$$\begin{aligned} \frac{\partial F}{\partial c_1} &= \int_{\Omega} \frac{\partial F}{\partial q} H(\phi) dx, & \frac{\partial F}{\partial c_2} &= \int_{\Omega} \frac{\partial F}{\partial q} (1 - H(\phi)) dx, \\ (13) \quad \frac{\partial F}{\partial \phi} &= (c_1 - c_2) \delta(\phi) \frac{\partial F}{\partial q}. \end{aligned}$$

In the above,  $\delta$  denotes the Dirac function, i.e.  $\delta(0) = 1$  and  $\delta(x) = 0, \forall x \neq 0$ . If we define  $\Omega_1 = \{x|x \in \Omega, \phi > 0\}$ ,  $\Omega_2 = \{x|x \in \Omega, \phi \leq 0\}$ , then it is easy to see that:

$$\frac{\partial F}{\partial c_1} = \int_{\Omega_1} \frac{\partial F}{\partial q} dx, \quad \frac{\partial F}{\partial c_2} = \int_{\Omega_2} \frac{\partial F}{\partial q} dx.$$

Now we consider the more general case of  $n$  level set functions as given in (11). From (11), we see that:

$$(14) \quad \frac{\partial q}{\partial c_i} = \prod_{j=1}^n R_i(\phi_j), \quad \frac{\partial q}{\partial \phi_i} = \sum_{i=1}^{2^n} c_i \left( \prod_{j=1, j \neq i}^n R_i(\phi_j) \right) D(\phi_i),$$

where

$$D(\phi_i) = \begin{cases} \delta(\phi_i), & \text{if } b_j^i = 0; \\ -\delta(\phi_i), & \text{if } b_j^i = 1. \end{cases}$$

Define  $\Omega_i$  to be the support set for  $\prod_{j=1}^n R_i(\phi_j)$ , i.e.

$$(15) \quad \Omega_i = \text{support of } \prod_{j=1}^n R_i(\phi_j).$$

It is easy to see that  $\Omega_i$  is the region that  $q = c_i$ . It can be seen that  $\partial q/\partial c_i$  is nonzero only in the region  $\Omega_i$  corresponding to  $q = c_i$ . Inside this region,  $\partial q/\partial c_i = 1$ . Correspondingly, we have that

$$(16) \quad \frac{\partial F}{\partial c_i} = \int_{\Omega_i} \frac{\partial F}{\partial q} dx.$$

In applications given later, we need to use the length of the curves as regularization functionals. The purpose of using this regularization term is to prevent the zero level curves becoming oscillatory. For gradient methods, we need to calculate the Gateaux differential for the length functional:

$$R(\phi_j) = \int_{\Omega} |\nabla H(\phi_j)| dx = \int_{\Omega} \delta(\phi_j) |\nabla \phi_j| dx.$$

To get the differential of  $R$  with respect to  $\phi_j$  in a direction  $\mu_j$ , we proceed

$$\frac{\partial R}{\partial \phi_j} \cdot \mu_j = \int_{\Omega} \delta'(\phi_j) \mu_j |\nabla \phi_j| dx + \int_{\Omega} \delta(\phi_j) \frac{\nabla \phi_j}{|\nabla \phi_j|} \cdot \nabla \mu_j dx.$$

Applying Greens formula to the last term which can be theoretically verified by replacing the delta function by a smooth function and then passing to the limit, we will get that

$$\begin{aligned}
& \frac{\partial R}{\partial \phi_j} \cdot \mu_j = \int_{\Omega} \delta'(\phi_j) \mu_j |\nabla \phi_j| dx - \int_{\Omega} \nabla \cdot \left( \delta(\phi_j) \frac{\nabla \phi_j}{|\nabla \phi_j|} \right) \mu_j dx \\
(17) \quad & = \int_{\Omega} \delta'(\phi_j) \mu_j |\nabla \phi_j| dx - \int_{\Omega} \left( \delta'(\phi_j) \frac{|\nabla \phi_j|^2}{|\nabla \phi_j|} \mu_j + \delta(\phi) \mu_j \nabla \cdot \frac{\nabla \phi_j}{|\nabla \phi_j|} \right) dx \\
& = - \int_{\Omega} \delta(\phi) \mu_j \nabla \cdot \frac{\nabla \phi_j}{|\nabla \phi_j|} dx,
\end{aligned}$$

which indicates that

$$(18) \quad \frac{\partial R}{\partial \phi_j} = -\delta(\phi_j) \nabla \cdot \frac{\nabla \phi_j}{|\nabla \phi_j|}.$$

**3.4. Smooth Approximations to  $H$  and  $\delta$  Functions.** In numerical implementations, it is desirable to replace the Heaviside function  $H$  and the delta function  $\delta$  by some smoothed counterparts. These epsilon-approximations are designed so that they are everywhere non-zero. This is useful for "growing" level sets in interior regions (e.g. inside of annular regions). Another clear motivation of using smoothed approximations is to get the involved functionals differentiable. In our simulations, the following smoothed functions for the Heaviside-function  $H$  and delta-function  $\delta$  have been used (c.f. [55]):

$$(19) \quad H_{\epsilon}(\phi) = \frac{1}{\pi} \tan^{-1} \frac{\phi}{\epsilon} + \frac{1}{2},$$

$$(20) \quad \delta_{\epsilon}(\phi) = \frac{\epsilon}{\pi(\phi^2 + \epsilon^2)}.$$

In order to have a good accuracy, we need to choose  $\epsilon$  sufficiently small. For small  $\epsilon$ ,  $\delta_{\epsilon}$  is a smooth function, but with very sharp singular layers. This makes it difficult to represent the  $\delta_{\epsilon}$  function in discretization. From our numerical experience, it was found that it is not good to use too small  $\epsilon$  for  $H_{\epsilon}$  and  $\delta_{\epsilon}$ .

However, there are also some other alternatives to deal with the singular function  $\delta(\phi)$ . For example, we can replace the  $\delta(\phi)$  function just by constant 1 or by  $|\nabla \phi|$  in the gradient and it can be proved that the direction is still a decent direction for some applications. For example, the decent direction used in [42, 31] are equal to replace  $\delta$  by 1 in our calculated derivatives. For many other applications considered in [40, 48], the decent directions are equal to replace the  $\delta$  function by  $|\nabla \phi|$  in our calculated derivatives. For some applications, replacing  $\delta(\phi)$  by  $|\nabla \phi|$  could accelerate the convergence of the resulting schemes and offer some other other advantages, see [38, p.392].

**3.5. Some new level set techniques without using  $H$  and  $\delta$  functions.**

Recently, different efforts have been devoted to develop efficient techniques to use level set methods to identify multiple phases without using the Heaviside and delta functions  $H$  and  $\delta$ , see [50, 34, 13, 33]. These techniques are able to decompose a domain into different subdomains. It is important that all the above mentioned techniques could automatically avoid overlaps and vacuum between the subdomains. Moreover, they also avoided the use of the the Heaviside and delta functions  $H$  and  $\delta$  so that no regularization is needed for these singular functions. The schemes of [50, 13] are fast and do not require gradient calculations during the iterations. Similarly to [55, 8], one can use  $k$  level set functions to identify  $2^k$  phases. The technique of

[34] is able to use just one level set function to identify arbitrary number of phases. Moreover, the associated minimization functional and the constraints involved are smooth. The level set function converges to a piecewise constant function. The method of [34] is not trying to move the interfaces during the iterations. Instead it is just trying to determine which point is inside a region and which point is outside a region using some minimization functionals under some constraint. This has some advantages in treating geometries, for example, in a situation where inside "holes" need to be identified. The method of [33] combines the advantages of both [50] and [34]. At convergence, the level set function converges to  $\pm 1$ , i.e. the level set functions satisfy  $\phi^2 = 1$ .

In the next few sections, we shall outline some problems where the multiple level set methods can be applied. These new level set techniques can be applied to these problems without any difficulties, even though we will only try to show applications of the approach outlined in section 3.1–3.4.

#### 4. Image segmentation

For some applications, we need to find the location of discontinuities for the intensity values of a given digital image and this process is often called image segmentation. One of such applications is the segmentation of images from medical magnetic resonance imaging (MRI). A typical MR image contains different regions and inside each region the image intensity value varies slowly. For clinical purposes, it is very important to accurately identify the boundary between the different regions. The thickness of some of the special regions give important information for doctors in practical clinical diagnosis.

Following [39], it was proposed in Chan and Vese [11, 12, 10, 9] that we can use piecewise constant functions (or higher order polynomials) to approximate the image functions. For one level set function, the minimization functional used in Chan and Vese [11, 12] is

$$(21) \quad G(c_i, \phi) = \int_{\Omega} \frac{1}{2} |c_1 - q_d|^2 H(\phi) dx + \int_{\Omega} \frac{1}{2} |c_2 - q_d|^2 (1 - H(\phi)) dx + \beta \int_{\Omega} |\nabla H(\phi)| dx.$$

It is easy to extend the above formulation to multiple level set functions, see [55].

If we use the general framework we have presented in section 3, we find that the Mumford-Shah minimization functional [39] can be written in the following form:

$$(22) \quad F(c_i, \phi_i) = \int_{\Omega} \frac{1}{2} |q - q_d|^2 dx + \beta \sum_i \int_{\Omega} |\nabla H(\phi_i)| dx.$$

Both (21) and (22) have been referred as the Chan-Vese model for segmentation problems. The formulation (22) bears more of the nature of the general formulation of [8, §3].

Using (12) and (18), it is easy to see that the differentials of  $F$  defined in (22) are given by:

$$\frac{\partial F}{\partial \phi_i} = (q - q_d) \frac{\partial q}{\partial \phi_i} - \beta \delta(\phi_i) \nabla \cdot \frac{\nabla \phi_i}{|\nabla \phi_i|}.$$

Let  $\Omega_i$  to be defined as in (15), we get from (12) that

$$\frac{\partial F}{\partial c_i} = \int_{\Omega} (q - q_d) \frac{\partial q}{\partial c_i} = c_i |\Omega_i| - \int_{\Omega_i} q_d dx.$$

In the above,  $|\Omega_i|$  denotes the measure of  $\Omega_i$ .

For one level set function, it is interesting to observe that  $F(c_i, \phi_i) = G(c_i, \phi_i)$  if we do not replace  $H$  by its smoothed counter part. However, the functional values of  $F$  and  $G$ , especially the derivatives  $\partial F/\partial \phi_i$  and  $\partial G/\partial \phi_i$ , are different if we use smoothed approximations for  $H$  and  $\delta$ . The following gradient algorithm have been used to find a minimizer for the functional (22):

**Algorithm 1.** *Determine how many level set functions we need to use. Choose initial level set functions  $\phi_i^0$  and the time step  $\Delta t$ . For  $k \geq 1$ ,*

- *Update the constant values by*

$$(23) \quad c_i^k = \int_{\Omega_i} q_d dx / |\Omega_i|.$$

- *Update the level set functions by*

$$(24) \quad \phi_i^k = \phi_i^{k-1} - \Delta t \frac{\partial F}{\partial \phi_i}(c_i^k, \phi_i^{k-1}).$$

- *If "necessary", reinitialize the level set functions  $\phi_i^k$ , i.e. set  $d_0 = \phi_i^k$ . Choose an appropriate  $\tau_0$  and solve equation (7) to  $t = \tau_0$ . The reinitialized  $\phi_i^k$  is then taken as*

$$(25) \quad \phi_i^k := d(x, \tau_0; \phi_i^k).$$

- *Update  $q^k$  as in the following and go to the next iteration:*

$$q^k = \sum_{i=1}^{2^n} c_i^k \prod_{j=1}^n R_i(\phi_j^k).$$

The above algorithm is essentially the same algorithm used in [55, 8]. As the functional (22) is quadratic with respect to  $c_i$ , we are trying to find the  $c_i$  values by enforcing  $\partial F/\partial c_i = 0$  in (23). The time step  $\Delta t$  in the gradient updating (24) is normally fixed or obtained by a line search. After some updating of  $\phi_i$  as in (24), the functions  $\phi_i$  are not distance functions any more. Thus, we try to project them back to be distance functions as in (25). However, it is suggested not to do this reinitialization very often. We shall reinitialize after a fixed number of updating or when the level set functions  $\phi_i$  have under-taken a sufficient amount of changes (for example, sufficiently many nodal values of  $\phi_i$  have changed sign). For some applications, we could recover the level set functions even without reinitialize the level set functions. There are different methods available in the literature for reinitialize the level set functions, see [40, 48, 47, 54, 56].

As the derivatives of the functional (22) differs from (21), we have tried to compare their numerical performances. Intensive numerical experiments have been done in Hodneland [28]. It seems that the scheme with (22) is more stable, otherwise the performance is nearly the same. We show some of the obtained results in the Figure 1. The numerical tests seem to indicate that it is better to use the total variational norm of  $\phi_i$  instead of length of the zero level curve of  $\phi_i$  as the regularization term. The results obtained have been compared with the widely used SPM (Statistical Parametrical Mapping, <http://www.fil.ion.ucl.ac.uk/spm>) algorithm. When the noise level is low, the level set method is as good as SPM. For higher level noise, the level set method gives better results [28], especially if the intensity value inside each region is inhomogeneous (i.e. the value is not nearly constant, but varies rather much), then the level set segmentation is much better.

In Algorithm 1, a gradient method is used to find the minimizer for the cost functional. We shall note that one can also use other methods to find the minimizer.

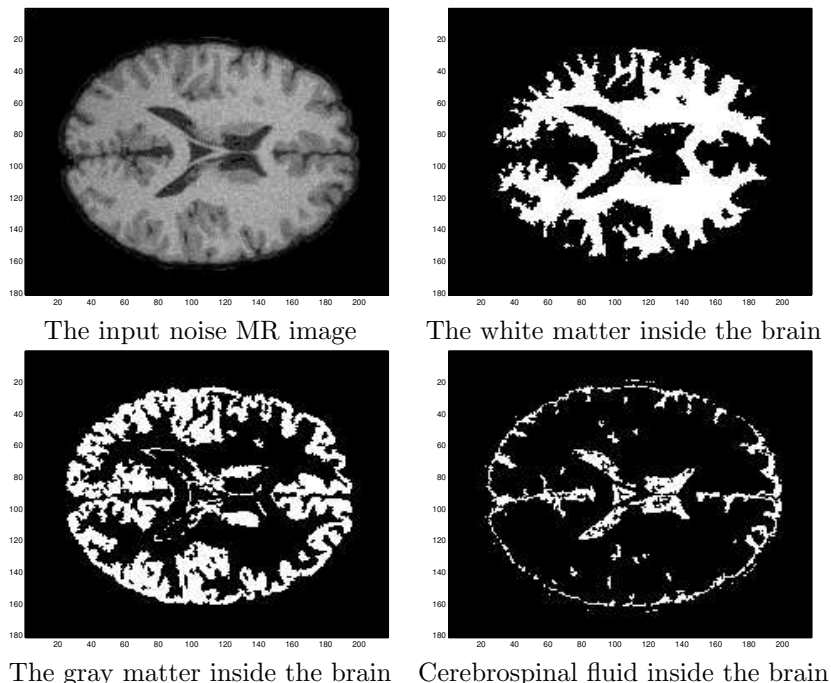


FIGURE 1. Segmentation of an MR brain image using functional (22).

See [27] for some recently developed fast methods for the level set segmentation. In a related survey paper [14], one could also find some more applications of the level set idea and variational PDE for image processing problems.

## 5. Optimal shape design problems

In applications, we often need to design shapes that minimize or maximize some given criteria. Some optimal shape design problems of such a kind can be formulated as identification problems for piecewise constant functions. The problem given in this section represents such a kind of optimal shape design problems and it is taken from Osher and Santosa [42], see also [4, 5, 46, 35] for some more problems that are similar in nature to what is given below.

Consider a drum head with a fixed shape  $\Omega \subset R^2$  and variable density  $q(x)$ . The resonant frequencies of the drum are found by solving the eigenvalue problem

$$-\Delta u = \lambda q(x)u, \quad x \in \Omega, \quad u = 0, x \in \partial\Omega.$$

Let  $S \subset \Omega$  be a domain inside  $\Omega$ . We do not assume any topology on  $S$ . We assume that the density  $q(x)$  takes on two values, i.e  $q(x) = c_1$  inside  $S$  and  $q(x) = c_2$  outside  $S$ . We will deal only with the first two eigenvalues  $\lambda_1$  and  $\lambda_2$ . It is known that  $\lambda_1$  and  $\lambda_2$  are distinct. The optimization problems we want to consider is to find the minimizers for

$$(26) \quad \max_S \lambda_1 \text{ or } \min_S \lambda_1 \text{ or } \max_S (\lambda_2 - \lambda_1).$$

subject to the constraint

$$|S| = c_0,$$

where  $|S|$  is the area of  $S$  and  $c_0$  is a prescribed number.

We use the Lagrange multiplier method to solve the optimization problem (26). For a given level set function  $\phi$  associated with  $S$ , let  $F(\phi) = \lambda_1$  or  $-\lambda_1$  or  $\lambda_2 - \lambda_1$  depending on the minimization property we want. Let  $G(\phi) = |S| - c_0 = \int_{\Omega} H(\phi) dx - c_0$  be the constraint function on the mass. The Lagrangian, with multiplier  $\nu$ , is given by

$$(27) \quad L(\phi, \nu) = F(\phi) + \nu G(\phi).$$

The necessary condition for a saddle point is

$$(28) \quad \frac{\partial L(\phi, \nu)}{\partial \phi} = \frac{\partial F(\phi)}{\partial \phi} + \nu \frac{\partial G(\phi)}{\partial \phi} = 0, \quad G(\phi) = 0.$$

In order to show how we calculate the gradient, we let for example  $F(\phi) = \lambda_1$ . Then, the eigenpair  $(u_1, \lambda_1)$  solves

$$(29) \quad -\Delta u_1 = \lambda_1 q(x) u_1, \quad x \in \Omega, \quad u_1 = 0, \quad x \in \partial\Omega.$$

Differentiating with respect to  $q$  in a direction  $\mu$  on both sides gives us:

$$-\Delta \left( \frac{\partial u_1}{\partial q} \cdot \mu \right) - \lambda_1 q(x) \left( \frac{\partial u_1}{\partial q} \cdot \mu \right) = q u_1 \left( \frac{\partial \lambda_1}{\partial q} \cdot \mu \right) + \lambda_1 \mu u_1.$$

Due to the reason that  $u_1$  is the eigenfunction for  $\lambda_1$ , it is easy to see that the left-hand side is orthogonal to  $u_1$ . Multiplying both sides with  $u_1$  and use (29), we get

$$\frac{\partial \lambda_1}{\partial q} \cdot \mu = - \frac{\lambda_1 \int_{\Omega} \mu u_1^2 dx}{\int_{\Omega} q(x) u_1^2 dx}.$$

Thus

$$\frac{\partial \lambda_1}{\partial q} = - \frac{\lambda_1 u_1^2}{\int_{\Omega} q(x) u_1^2 dx}.$$

Using the chain rule (12), it is easy to get  $\partial \lambda_1 / \partial \phi$ . From the fact that  $\partial G / \partial \phi = \delta(\phi)$ , we easily can derive the formula for  $\partial L / \partial \phi$ . Once the gradient is known, one can use a gradient method of Uzawa type or projected gradient method to find a saddle point for the Lagrangian  $L$ .

Before we conclude, we just want to emphasize that the results we have presented above in this section is completely due to [42]. We just want to show that we can formulate their problem and approach in the general level set formulation we have presented. The gradient calculation we have given above is also essentially the same as the one given in [42]. In [42], they try to find a decent direction. The decent direction they got is equivalent to replace the  $\delta$  function in our gradient by constant 1. See [42] for some intensive numerical tests for this optimal shape design problem.

## 6. An elliptic inverse problem

Consider the partial differential equation:

$$(30) \quad \begin{cases} -\nabla \cdot (q(x) \nabla u) = f & \text{in } \Omega \subset R^2, \\ u = 0 & \text{on } \partial\Omega. \end{cases}$$

We want to use observations of the solution  $u$  to recover the coefficient  $q(x)$  which is assumed to be piecewise constant. This is a typical example for ill-posed problems. A small error in the observation for the state variable  $u$  could produce a large error in the recovered coefficient  $q(x)$ . Even as a purely academic problem, this seemingly simple problem is rather difficult to solve by numerical schemes. In the presence of noise in the observation data, it has been shown theoretically, c.f. [23, 24, 51, 52, 53], that the approximation error increases as the mesh size decreases. Up to now, it

seems that there are not many available algorithms that can solve this inverse problem with relatively large noise on a sufficient fine mesh.

The desire to recover accurately the geometry of the coefficient discontinuities have motivated a number of approaches in the literature [6, 7, 15, 3, 25, 16]. One approach is to use a regularization of the coefficient which respects the jumps and the geometry of the discontinuities. For example, in our earlier work [6, 7], the Total Variation norm regularization technique is combined with the augmented Lagrangian technique of [29, 32] for this purpose. Other works along this line are [16, 15], etc. An alternative approach is to model the geometry of the discontinuities implicitly in the representation of the coefficient. Specifically, several approaches using level set ideas have been recently proposed for this purpose; see [31, 4, 5, 21, 27] for some pioneering work in this direction. In Ito-Kunisch-Li [31], level set ideas are used for elliptic inverse problems similar to the ones we are considering in this paper. Another related work is Ben Ameur-Chavent-Jaffré [1]. In [1], piecewise constants are used to approximate the coefficient and they try to adaptively refine the mesh until some given criteria are met. For our level set approach, we use a fixed fine mesh, but we use the level set functions to find the best partition of the domain into piecewise constant regions to give a best match for the measurement.

Due to the ill-posedness of the problem, output-least-squares method is often used for recovering  $q(x)$ . Assume that  $u_d$  is an observation for  $u$ , the minimization functional for the output-least-squares method is:

$$(31) \quad F = \int_{\Omega} \frac{1}{2} |u - u_d|^2 dx + \beta \int_{\Omega} |\nabla q| dx.$$

In the above,  $u$  is the solution of (30) with a given  $q$  and  $\int_{\Omega} |\nabla q| dx$  is the total variation norm of  $q$ . In case we only have a sparse observation or other kind of observations for  $u$ , the modifications needed for the numerical scheme is minor. We shall use level set method to represent the coefficient  $q(x)$ . So the function  $q(x)$  depends on the level set functions  $\phi_i$  and the constant values  $c_i$ . From the chain rule (12), we just need to calculate  $\partial F / \partial q$  in order to get  $\partial F / \partial \phi_i$  and  $\partial F / \partial c_i$ . Differentiating with respect to  $q$  in a direction  $\mu$  for equation (30), we get that

$$(32) \quad -\nabla \cdot \left( q(x) \nabla \left( \frac{\partial u}{\partial q} \cdot \mu \right) \right) - \nabla \cdot (\mu \nabla u) = 0.$$

In the above,  $\frac{\partial u}{\partial q} \cdot \mu$  denotes the derivative of  $u$  in a direction  $\mu$  at a given  $q$ . The precise definition of this derivative can be given as:

$$(33) \quad \frac{\partial u}{\partial q} \cdot \mu = \lim_{\epsilon \rightarrow 0} \frac{u(q + \epsilon \mu) - u(q)}{\epsilon}.$$

For general problem, the limit above is related to a proper norm. For this concrete problem, the limit above is understood in the norm of  $H_0^1(\Omega)$ .

Define  $z(x) \in H_0^1(\Omega)$  to be the solution of

$$(34) \quad -\nabla \cdot (q(x) \nabla z) = u - u_d \text{ in } \Omega, \quad z = 0 \text{ on } \partial\Omega.$$

From the variational forms for the weak solutions for (32) and (34), it is easy to get that

$$\begin{aligned} \frac{\partial F}{\partial q} \cdot \mu &= \int_{\Omega} \left( (u - u_d) \left( \frac{\partial u}{\partial q} \cdot \mu \right) + \beta \frac{\nabla q \cdot \nabla \mu}{|\nabla q|} \right) dx \\ &= \int_{\Omega} \left( \mu \nabla u \cdot \nabla z + \beta \frac{\nabla q \cdot \nabla \mu}{|\nabla q|} \right) dx. \end{aligned}$$

Again,  $\frac{\partial F}{\partial q} \cdot \mu$  above is the directional derivative of  $F$  which could be defined similarly as in (33). From the above, we get that

$$\frac{\partial F}{\partial q} = -\nabla u \cdot \nabla z - \beta \nabla \cdot \left( \frac{\nabla q}{|\nabla q|} \right).$$

In order to compute  $\partial F / \partial q$  once, we need to solve both equations (30) and (34) once. The following algorithm could be used to recover the coefficient  $q(x)$ :

**Algorithm 2.** *Determine how many level set functions we need to use. Choose initial level set functions  $\phi_i^0$ , constant values  $c_i^0$ . For  $k \geq 1$ ,*

- Update  $q^k$  by

$$q^k = \sum_{i=1}^{2^n} c_i^{k-1} \prod_{j=1}^n R_i(\phi_j^{k-1}).$$

- Compute  $u^k$  and  $z^k$  from equations (30) and (34).
- Choose the step size  $\alpha_i^n$  and update the constant values by

$$c_i^k = c_i^{k-1} - \alpha_i^n \int_{\Omega_i} \frac{\partial F}{\partial q}(q^k, z^k, u^k) dx.$$

- Choose the step size  $\sigma_i^n$  and update the level set functions as:

$$\phi_i^k = \phi_i^{k-1} - \sigma_i^n \frac{\partial F}{\partial q}(q^k, z^k, u^k) \frac{\partial q}{\partial \phi_i}(c_i^k, \phi_i^{k-1}).$$

- If "necessary", reinitialize the level set functions  $\phi_i^k$ , i.e. set  $d_0 = \phi_i^k$ . Choose an appropriate  $\tau_0$  and solve equation (7) to  $t = \tau_0$ . The reinitialized  $\phi_i^k$  is then taken as

$$(35) \quad \phi_i^k := d(x, \tau_0; \phi_i^k).$$

- Go to the next iteration if not converged.

Similar to image segmentation, the reinitialization step (35) should not be done very often. The above algorithm differs from the algorithm of Chan and Tai [26, 8]. In Chan and Tai [26, 8], augmented Lagrangian method was used to enforce the equation constraint (30). The cost per iteration for the above algorithm is somehow more expensive than the augmented Lagrangian approach. However, the above algorithm seems to be more stable with respect to initial guess and converges faster when the iterative solution is still far from the true solution. For numerical purpose, the details explained in [8] for calculating the gradients and the other technical devices are all relevant for the above scheme. The step sizes  $\alpha_i^n$  and  $\sigma_i^n$  could be fixed during the iterations. One can also use a line search to find the step sizes. To guarantee that the recovered  $q$  is positive, we assume that the constant values  $c_i \in [a_i, b_i]$  and  $a_i, b_i$  are known a priori. One test example is shown in Figure 2 and 3. The true coefficient, solution  $u$  and the curve for the discontinuity is shown in Figure 2. The identified coefficient and the curve for different iterations are shown in Figure 3. In the test, we have used  $\Omega = [0, 1] \times [0, 1]$ , mesh size  $h = 1/64$ ,  $\beta = 5 \times 10^{-6}$ , times steps  $\alpha_i^n = 0.01, \sigma_i^n = 5$ . The  $\epsilon$  value used for  $H_\epsilon$  and  $\delta_\epsilon$  is  $\epsilon = h$ . With 1% noise in the observation, it is remarkable to see that the algorithm is able to recover the concave part of the curves and the sharp corners of the curves are also captured rather well. Note especially that the region inside the concave part of the curve on the left side is very thin and the algorithm is still able to identify this region rather accurately.

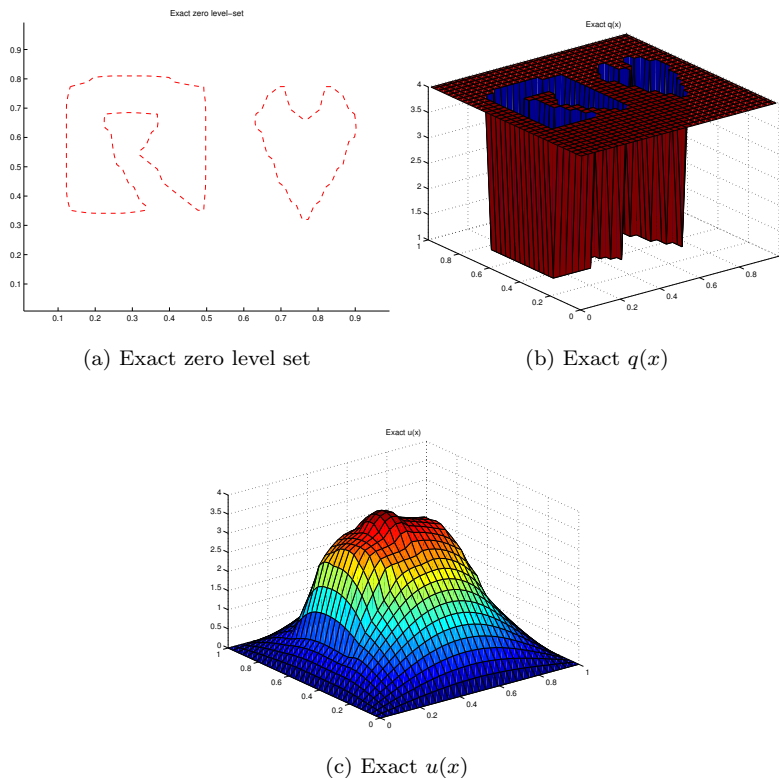


FIGURE 2. The exact  $q(x)$  and the location of the discontinuity

## 7. Electrical impedance tomography

There are a variety of medical problems for which it would be useful to know the time-varying distribution of electrical properties inside a human body [2, 17, 20, 45]. One way to identify the electrical properties inside the body is to apply some current with some low angular frequencies. This will produce a magnetic field inside the body. Under the condition that the angular frequency and the conductivity are low, one can get from the Maxwell's equation that the electric potential  $u$  in the body is governed by the equation

$$(36) \quad \nabla(q(x, \omega)\nabla u) = 0.$$

Here  $u$  is the electric potential or voltage, and  $\omega$  is the angular frequency of the applied current which is assumed to be fixed for the setting of the problem. Instead of reducing the Maxwell's equation to the elliptic equation (36), one can also try to reduce it to the Helmholtz equation as in [21]. In practice, we apply currents to electrodes on the surface of the body. These currents produce a current density on the surface whose inward pointing normal component is known. The current will produce some electric potentials which we shall measure on the surface of the human body. Mathematically, we say that we have  $N$  functions  $g_i$  defined on the surface  $\partial\Omega$ . This will produce  $N$  solutions to (36), i.e.

$$(37) \quad \nabla(q(x)\nabla u_i) = 0 \text{ in } \Omega, \quad \frac{\partial u_i}{\partial n} = g_i.$$

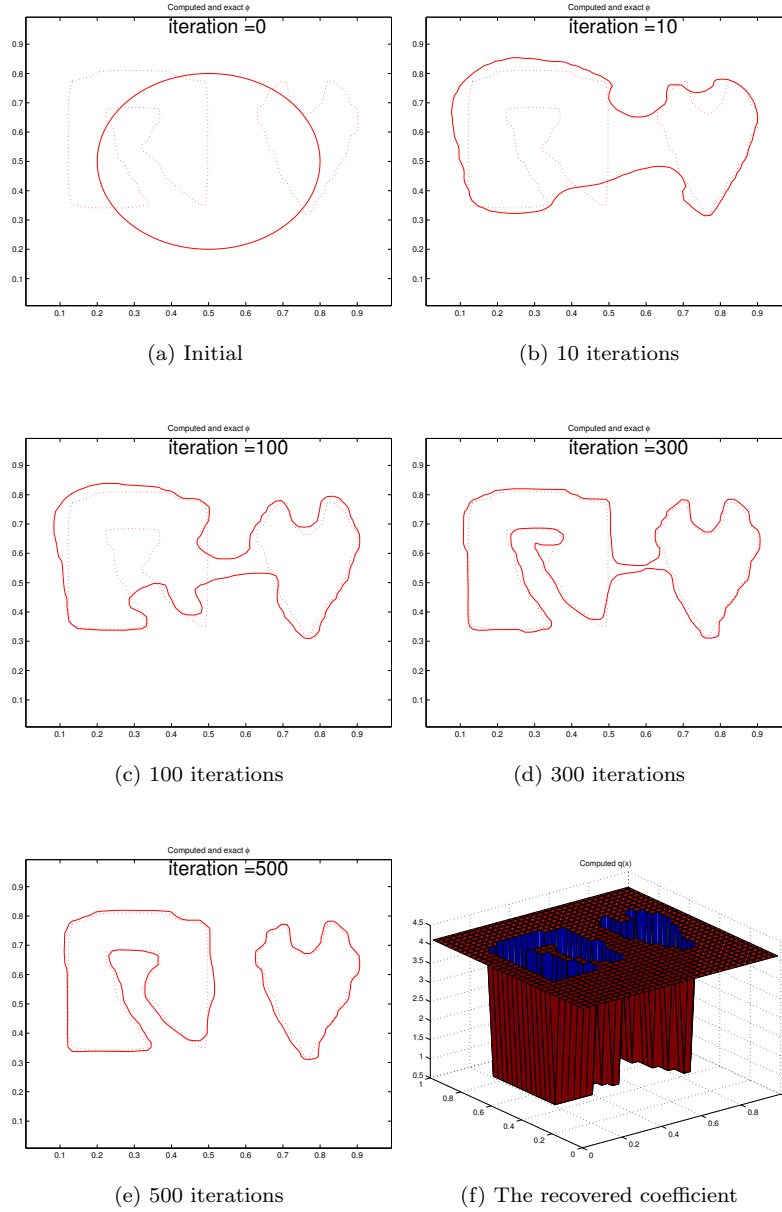


FIGURE 3. The identified zero level curve with 1% noise. The initial curve is a circle. It automatically splits into two separated regions during the iterations.

We assume that we have measured the values of  $u_i$  on  $\partial\Omega$ , i.e. we have measurements  $m_i = u_i|_{\partial\Omega}$ . We shall use  $m_i$  to recover a piecewise constant  $q(x)$ . For physical reasons, we need to require that

$$\int_{\partial\Omega} u_i ds = 0, \quad \int_{\partial\Omega} g_i ds = 0.$$

We shall use the output-least-squares method similarly as in [17, 20, 45] to find  $q$ . The minimization functional is

$$F(q) = \frac{1}{2} \sum_{i=1}^N \int_{\partial\Omega} |u_i(q) - m_i|^2 ds + \beta \int_{\Omega} |\nabla q| dx.$$

For a given  $q$ , let  $u_i = u_i(q)$  be the corresponding solution of (37) and define  $z_i$  be the solutions of

$$\begin{aligned} -\nabla \cdot (q \nabla z_i) &= 0 \quad \text{in } \Omega \\ q \frac{\partial z_i}{\partial n} &= u_i - m_i \quad \text{on } \partial\Omega, \quad \int_{\partial\Omega} z_i ds = 0. \end{aligned}$$

it can be shown that

$$\frac{dF}{dq} = - \sum_{i=1}^N \nabla u_i \cdot \nabla z_i - \beta \nabla \cdot \left( \frac{\nabla q}{|\nabla q|} \right).$$

See Chung, Chan and Tai [18] for the details. Once we get  $\partial F/\partial q$ , it is easy to use (12) to get  $\partial F/\partial \phi_i$  if we represent  $q$  using level set functions as in (11). An algorithm similar to Algorithm 2 could be used to update the level set functions  $\phi_i^k$  and the constant values  $c_i^k$ . In Figure 4, we present some numerical results with 4, 12 and 60 observations. The observations contain 1% of noise. The dotted line shows the true discontinuity. The solid line is the recovered discontinuity. More measurements give a better accuracy for the recovered curve. Compared with other approaches, it seems that our algorithm is more robust with respect to noise.

## 8. Positron Emission Tomography

In PET (positron emission tomography), a compound containing a radiative isotope is injected into a human body and forms an unknown emission density  $q(x) \geq 0, x \in \Omega$ . The positron emitted finds a nearby electron and annihilates into two photons. The two photons travels at almost opposite directions. A detector ring surrounds the patient and collects all emissions. For an emission event to be counted, both photons must be registered nearly simultaneously at two opposite detectors. Regions with higher concentration of radioactivity causes a higher emission rate. Given the total number of measured counts at each detector pair, the challenge is to locate all emission sources inside the detector ring (c.f. [36, 30]). Mathematically, the recovery of  $q(x)$  can be formulated in the following way. First, we cover the domain  $\Omega$  by a uniform square mesh. Assume the squares are indexed by  $i = 1, 2, \dots, B$  and  $q(x)$  is a constant  $q_i$  inside each square. The detector pairs are indexed by  $j = 1, 2, \dots, T$ . If there are  $k$  detectors, we can have maximumly  $k(k-1)/2$  detector pairs, i.e.  $T \leq k(k-1)/2$ . The two photons emits in two random directions. For a given intensity  $q(x)$ , the maximum probable measurement we get is  $\vec{n} = P\vec{q}$ , where  $\vec{n} = \{n_j\}_{j=1}^T$  and  $\vec{q} = \{q_i\}_{i=1}^B$  is the vector for  $q$ . The detection probability matrix  $P$  is given, see [36, 30] for some details about how to get the matrix  $P$ .

Based on some statistical arguments, it turns out that we need to solve the following minimization problem in order to find a  $q$  for a given measurement  $\vec{n}$ :

$$(38) \quad \min_{\vec{q}} F(\vec{q}), \quad F(\vec{q}) = \left( \sum_{i=1}^B q_i - \sum_{j=1}^T n_j \log(P\vec{q})_j \right).$$

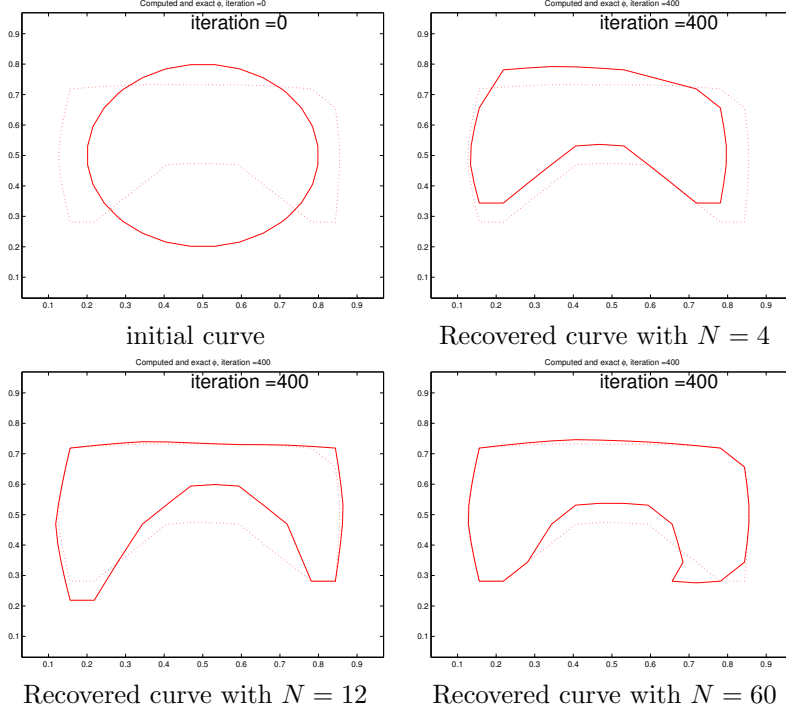


FIGURE 4. Recovered discontinuity using different number of boundary measurements. More measurements give a better accuracy for the recovered curve.

We can see that the gradient of  $F(\vec{q})$  is given by:

$$\frac{\partial F}{\partial \vec{q}} = e - P^t(\vec{n}./P\vec{q}).$$

In the above,  $e$  is the vector whose elements are all 1,  $P^t$  is the transpose of  $P$  and  $(\vec{n}./P\vec{q})$  is the elementwise division of vector  $\vec{n}$  by vector  $P\vec{q}$ . We assume the  $q$  is piecewise constant, i.e. the  $q_i$  values may equal to the same constant for many elements inside a given region, and thus can be represented by the level set representation shown in §3. Let  $\vec{\phi} = \{\phi_k\}_{k=1}^B$  be the vector for the values for a given level set function  $\phi$  over the squared elements. Using chain rule (12), it is easy to see that

$$\frac{\partial F}{\partial c_k} = h^2 \sum_{i=1}^B \frac{\partial F}{\partial q_i} \frac{\partial q_i}{\partial c_k}, \quad \frac{\partial F}{\partial \phi_k} = \frac{\partial F}{\partial q_k} \frac{\partial q_k}{\partial \phi_k}.$$

In the above,  $h$  is the mesh size. If we need more than one level set function, we just need to calculate the gradient similarly for each level set function. Once the gradients are known, we can use an algorithm similar to Algorithm 2 to update the level set functions and the constant values.

In Figures 5 and 6, we present one test example with a synthetic data set. For this example, the true  $\lambda$  has three regions. The constant values are assumed to be known. In the computation, we perturb the constant values by 10% and then fix them during the iterations. The initial level set functions give four regions. The

extra region disappears during the iterations. The recovered and the true  $\lambda$  are shown in Figure 5 and the evolution of the level set functions are shown in Figure 6. We refer to [36] for more numerical experiments.

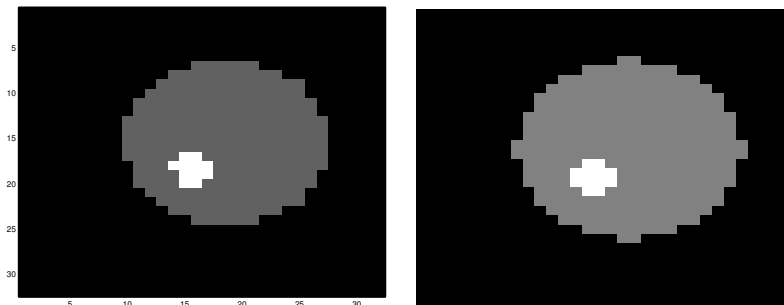


FIGURE 5. The recovered and the true  $\lambda$  function. Left: recovered; Right: true.

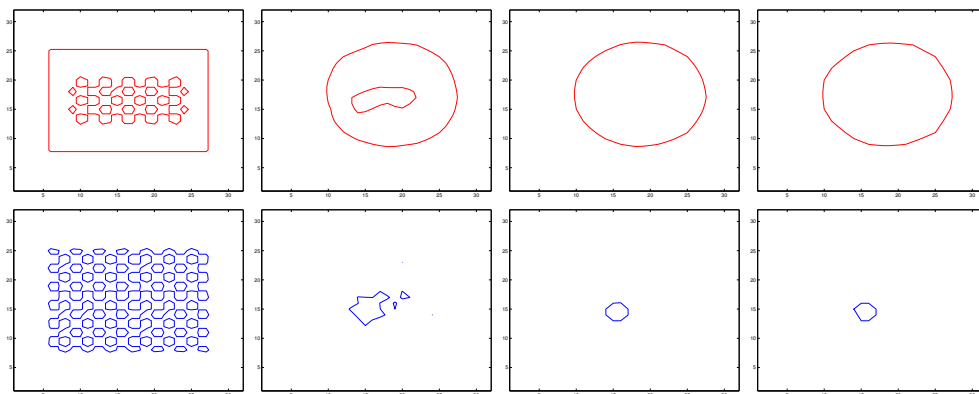


FIGURE 6. Evolutions of the two level set functions. From left to right: initial level set functions, 50, 150 and 650 iterations.

## 9. Other applications in brief

The level set method is designed to trace moving interfaces, thus it is natural to use it for different kind of free boundary problems related to partial differential equations. See [41, 49] for some application to Stefan type of problems, [46] for constructing obstacles, [44, 57] for some other applications. However, for some free boundary problems, we need to consider some variants of the level set idea in order to use the level set function with the partial differential equations for free boundary problems. Consider a model free boundary problem which comes from minimization problem (1) with:

$$(39) \quad F(v) = \int_{\Omega} \frac{1}{2} |\nabla v|^2 - fv, \quad K = \{v \mid v \in H_0^1(\Omega), v \geq \psi\}.$$

In the above  $\psi$  is the obstacle function and  $\psi \leq 0$  on  $\partial\Omega$ . The solution  $u$  for (39) is unique and it can be formally written as the function satisfying

$$-\Delta u \geq f, \quad u \geq \psi, \quad (-\Delta u - f) \cdot (u - \psi) = 0.$$

To find the solution  $u$ , we need to find the contact region  $\Omega^+ = \{x \mid u(x) = \psi(x), x \in \Omega\}$ . Once we know  $\Omega^+$ , the value of  $u$  in  $\Omega \setminus \Omega^+$  can be obtained from solving

$$-\Delta u = f \text{ in } \Omega \setminus \Omega^+, \quad u = 0 \text{ on } \partial\Omega, \quad u = \psi \text{ on } \partial\Omega^+.$$

In order to find  $u$ , we essentially just need to find  $\Gamma = \partial\Omega^+$ . Inside  $\Gamma$ ,  $u = \psi$  and outside  $\Gamma$ ,  $u$  is the solution of the Poisson equation.

It is not easy to use the level set idea sketched in §3.1 directly for this free boundary problem. However, we note that for any  $v \in K$ , there exists a  $\phi \in H_0^1(\Omega)$  (may not be unique) such that

$$(40) \quad a). \ v = \psi + \phi H(\phi), \quad \text{or} \quad b). \ v = \psi + \phi + |\phi|.$$

For any given  $\phi$ , let  $v = v(\phi)$  to be one of the two representations given in (40). We shall consider the following minimization problem:

$$(41) \quad \min_{\phi \in H_0^1(\Omega)} F(v(\phi)).$$

If  $\phi$  is a solution for (41), then  $v(\phi)$  is a solution for (1) with  $F$  and  $K$  given in (39). However, we shall note that the minimizer for (40) is not unique. If we replace  $H(\phi)$  by  $H_\epsilon(\phi)$  or replace  $|\phi|$  by  $\phi/\sqrt{\phi^2 + \epsilon}$ , then the minimization problem (40) has a unique solution. Using the chain rule (12), it is easy to calculate that the derivatives with representation (40.a) and (40.b) and they are given respectively by

$$(42) \quad a). \quad \frac{\partial F}{\partial \phi} = \frac{\partial F}{\partial v} \frac{\partial v}{\partial \phi} = (-\Delta v - f)(H_\epsilon(\phi) + \phi \delta_\epsilon(\phi)).$$

$$(43) \quad b). \quad \frac{\partial F}{\partial \phi} = \frac{\partial F}{\partial v} \frac{\partial v}{\partial \phi} = (-\Delta v - f) \left( 1 + \frac{\phi}{\sqrt{\phi^2 + \epsilon}} \right).$$

In simulations, the functions are approximated by discretized functions with a given mesh size. We need to choose  $\epsilon$  properly so that the error introduced by  $\epsilon$  is comparable with the discretization error, see Majava and Tai [37] for the details about the analysis and some numerical experiments. In Figure 7 and 8, we show some of the experimental results taken from Majava and Tai [37]. The results are produced using the gradient methods  $\phi^{n+1} = \phi^n - \alpha \partial F / \partial \phi(\phi^n)$  and with a fixed step size  $\alpha$ . We take  $\epsilon = h^2$  for (42) and  $\epsilon = h^4$  for (43). The step size is taken to be  $\alpha = 10^{-4}$  or  $\alpha = 10^{-5}$  and we have not tried to optimize  $\alpha$ .

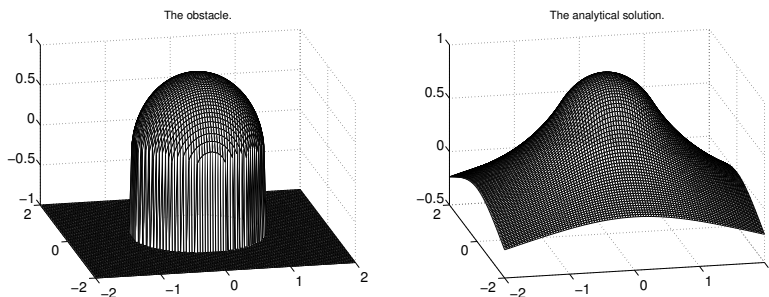


FIGURE 7. The obstacle and the analytical solution  $u$ .

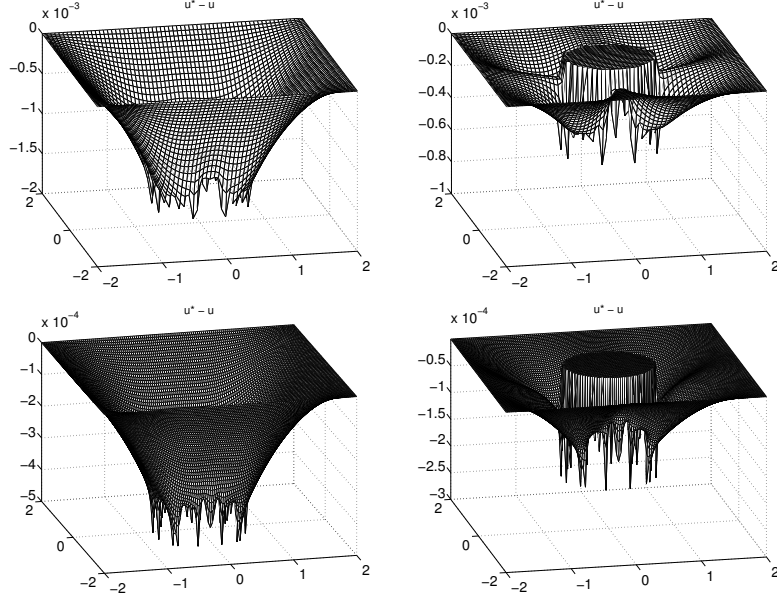


FIGURE 8. Errors between the obtained result  $u^*$  and the analytical solution  $u$ . Top:  $65 \times 65$  grid points; bottom:  $129 \times 129$  grid points. Left: results using (42) and gradient decent method, right: results using (43) and gradient decent method

## 10. Conclusions

There are many applications that we need to find the minimizer of a cost functional with respect to piecewise constant functions. We have illustrated how to use multiple level sets to represent piecewise constant functions. A uniform, powerful and general framework for solving a wide variety of inverse problems and optimization problems are given in this work. It is assumed that the recovered function is constant inside each region. It is easy to extend the idea to case that the recovered function is a polynomial of a given order inside each region.

## 11. Appendix

In this appendix, we give a brief account about the chain's rules in (12). Under proper assumptions on  $F$  and its derivatives, it is true that the following Taylor expansion is correct:

$$(44) \quad F(q + \mu) - F(q) = \int_{\Omega} G(q)\mu dx + o(\|\mu\|)\|\mu\|.$$

In the above,  $\|\mu\|$  is a proper norm for  $\mu$ . If  $q$  is represented using the level set functions as in (11), then  $q$  is a function of the level set functions  $\phi_i$  and the constant values  $c_i$ , i.e.

$$q = q(\phi_i, c_i).$$

If we perturb the value of  $c_i$  by  $\epsilon_i$  and define  $\mu_i = q(\phi_i, c_i + \epsilon_i) - q(\phi_i, c_i)$ , it is easy to get the following relation from (44):

$$(45) \quad \frac{F(q(\phi_i, c_i + \epsilon_i)) - F(q(\phi_i, c_i))}{\epsilon_i} = \int_{\Omega} G(q + \mu_i) \frac{\mu_i}{\epsilon_i} dx + o(\|\mu_i\|) \left\| \frac{\mu_i}{\epsilon_i} \right\|.$$

Assuming that  $G(\cdot)$  is continuous and also noting that

$$\lim_{\epsilon_i \rightarrow 0} \frac{\mu_i}{\epsilon_i} = \frac{\partial q}{\partial c_i},$$

we get the first formula in (12) by letting  $\epsilon_i \rightarrow 0$  and using (45). The second formula in (12) is also easy to derive from (44) just if the needed continuity assumptions are valid for  $F$  and its derivatives.

## 12. Acknowledgment

The authors thank Eric Chung, Erlend Hodneland, Marius Lysaker and Kirsi Majava for pleasant collaborations and for providing some of the numerical results for this paper.

## References

- [1] H. Ben Ameur, G. Chavent, and J. Jaffré. Refinement and coarsening indicators for adaptive parametrization: application to the estimation of hydraulic transmissivities. *Inverse Problems*, 18:775–794, 2002.
- [2] Martin Brühl and Martin Hanke. Numerical implementation of two noniterative methods for locating inclusions by impedance tomography. *Inverse Problems*, 16(4):1029–1042, 2000.
- [3] Kari Brunstad and Trond Mannseth. Basis norm rescaling for nonlinear parameter estimation. *SIAM J. Sci. Comput.*, 21(6):2114–2125 (electronic), 2000.
- [4] M. Burger. A level set method for inverse problems. *Inverse problems*, 17:1327–1356, 2001.
- [5] M. Burger. A framework for the construction of level set methods for shape optimization and reconstruction. *Interfaces and Free boundaries*, 5:301–329, 2005.
- [6] T. F. Chan and X.-C. Tai. Augmented lagrangian and total variation methods for recovering discontinuous coefficients from elliptic equations. In M. Bristeau, G. Etgen, W. Fitzgibbon, J. L. Lions, J. Periaux, and M. F. Wheeler, editors, *Computational Science for the 21st Century*, pages 597–607. John Wiley & Sons, 1997.
- [7] T. F. Chan and X.-C. Tai. Identification of discontinuous coefficients in elliptic problems using total variation regularization. *SIAM J. Sci. Comput.*, 25:881–904, 2003. Available online at <http://www.mi.uib.no/~tai/>.
- [8] T. F. Chan and X.-C. Tai. Level set and total variation regularization for elliptic inverse problems with discontinuous coefficients. *J. Comput. Phys.*, 193:40–66, 2003.
- [9] T. F. Chan and L. A. Vese. Image segmentation using level sets and the piecewise constant mumford-shah model. Technical report, CAM Report 00-14, UCLA, Math. Depart., April 2000. revised December 2000.
- [10] T.F. Chan, B.Y. Sandberg, and L.A. Vese. Active contours without edges for vector-valued images. *UCLA CAM report 99-35*, 1999.
- [11] T.F. Chan and L.A. Vese. Variational image restoration and segmentation models and approximations. *UCLA CAM report 97-47*, 1997.
- [12] T.F. Chan and L.A. Vese. Active contours without edges. *IEEE Trans. Image Processing*, 10:266–276, 2001.
- [13] Tony F. Chan and Selim Esedoglu. A multiscale algorithm for mumford-shah image segmentation. *UCLA, CAM-report 03-77*, 2003.
- [14] Tony F. Chan, Jianhong Shen, and Luminita Vese. Variational PDE models in image processing. *Notices Amer. Math. Soc.*, 50(1):14–26, 2003.
- [15] G. Chavent and K. Kunisch. Regularization of linear least squares problems by total bounded variation. *ESAIM Control Optim. Calc. Var.*, 2:359–376 (electronic), 1997.
- [16] Zhiming Chen and Jun Zou. An augmented Lagrangian method for identifying discontinuous parameters in elliptic systems. *SIAM J. Control Optim.*, 37(3):892–910 (electronic), 1999.
- [17] Margaret Cheney, David Isaacson, and Jonathan C. Newell. Electrical impedance tomography. *SIAM Rev.*, 41(1):85–101 (electronic), 1999.
- [18] E. T. Chung, T. F. Chan, and X.-C. Tai. A level set method for electrical impedance tomography. *UCLA, CAM-report 03-64*, 2003.
- [19] Michael G. Crandall, Hitoshi Ishii, and Pierre-Louis Lions. User’s guide to viscosity solutions of second order partial differential equations. *Bull. Amer. Math. Soc. (N.S.)*, 27(1):1–67, 1992.

- [20] D. C. Dobson and F. Santosa. An image enhancement technique for electrical impedance tomography. *Inverse problems*, 10:317–334, 1994.
- [21] O. Dorn, E. M. Miller, and C. M. Rappaport. A shape reconstruction method for electromagnetic tomography using adjoint and level sets. *Inverse problems*, 16:1119–1156, 2000.
- [22] I. Ekeland and R. Temam. *Convex analysis and variational problems*. North-Holland, Amsterdam, 1976.
- [23] Richard E. Ewing, Tao Lin, and Yanping Lin. A mixed least-squares method for an inverse problem of a nonlinear beam equation. *Inverse Problems*, 15(1):19–32, 1999. Conference on Inverse Problems, Control and Shape Optimization (Carthage, 1998).
- [24] Richard S. Falk. Error estimates for the numerical identification of a variable coefficient. *Math. Comp.*, 40(162):537–546, 1983.
- [25] Alv-Arne Grimstad, Trond Mannseth, Geir Nævdal, and Hege Urkedal. Adaptive multiscale permeability estimation. *Comput. Geosci.*, 7(1):1–25, 2003.
- [26] B. Heimsund, T. F. Chan, T. K. Nilssen, and X.-C. Tai. Level set methods and augmented lagrangian for a parameter identification problem. In V. Barbu, I. Lasiecka, D. Tiba, and C. Varsan, editors, *Analysis and optimization of differential systems*, pages 189–200. Kluwer Academic Publishers, Boston/Dordrecht/London, 2003.
- [27] Michael Hintermüller and Wolfgang Ring. A second order shape optimization approach for image segmentation. *SIAM J. Appl. Math.*, to appear.
- [28] Erlend Hodneland. Segmentation of digital images. Cand. scient thesis, Department of Mathematics, University of Bergen, 2003. Available online at <http://www.mi.uib.no/%7Eetai>.
- [29] K. Ito and K. Kunisch. The augmented lagrangian method for parameter estimation in elliptic systems. *SIAM J. Control Optim.*, 28:113–136, 1990.
- [30] E. Jonsson, S. C. Huang, and T. F. Chan. Total variation regularization in positron emission tomography. <http://www.math.ucla.edu/applied/cam/index.html>, UCLA, CAM-report 98-48:1–25, 1998.
- [31] K. Ito, K. Kunisch, and Z. Li. Level-set function approach to an inverse interface problem. *Inverse Problems*, 17:1225–1242, 2001.
- [32] K. Kunisch and X.-C. Tai. Sequential and parallel splitting methods for bilinear control problems in Hilbert spaces. *SIAM J. Numer. Anal.*, 34:91–118, 1997.
- [33] Johan Lie, Marius Lysaker, and Xue-Cheng Tai. A binary level set model and some applications to image segmentation. *UCLA, CAM-report*, 2004.
- [34] Johan Lie, Marius Lysaker, and Xue-Cheng Tai. A variant of the level set method and applications to image segmentation. *UCLA, CAM-report 03-50*, September, 2003.
- [35] A. Litman, D. Lesselier, and F. Santosa. Reconstruction of a two dimensional binary obstacle by control evolution of a level set. *inverse problems*, 14:685–706, 1998.
- [36] M. Lysaker, T. F. Chan, and X.-C. Tai. Level set method for positron emission tomography. *UCLA CAM-report*, 2004.
- [37] K. Majava and X.-C. Tai. A variant of the level set methods for obstacle problems. *International J. Numer. Anal. Modelling*, 1, 2004.
- [38] Antonio Marquina and Stanley Osher. Explicit algorithms for a new time dependent model based on level set motion for nonlinear deblurring and noise removal. *SIAM J. Sci. Comput.*, 22(2):387–405 (electronic), 2000.
- [39] D. Mumford and J. Shah. Optimal approximation by piecewise smooth functions and associated variational problems. *Comm. Pure Appl. Math.*, 42:577–685, 1989.
- [40] S. Osher and R. Fedkiw. *Level set methods and dynamic implicit surfaces*, volume 153 of *Applied Mathematical Sciences*. Springer-Verlag, New York, 2003.
- [41] S. Osher and R. P. Fedkiw. Level set methods: an overview and some recent results. *J. Comput. Phys.*, 169(2):463–502, 2001.
- [42] S. Osher and F. Santosa. Level set methods for optimization problems involving geometry and constraints. I. Frequencies of a two-density inhomogeneous drum. *J. Comput. Phys.*, 171(1):272–288, 2001.
- [43] S. Osher and J. A. Sethian. Fronts propagating with curvature dependent speed: Algorithms based on hamilton-jacobi formulations. *J. Comput. Phys.*, 79:12–49, 1988.
- [44] Danping Peng, Barry Merriman, Stanley Osher, Hongkai Zhao, and Myungjoo Kang. A PDE-based fast local level set method. *J. Comput. Phys.*, 155(2):410–438, 1999.
- [45] L. Rondi and F. Santosa. Enhanced electrical impedance tomography via the mumford-shah functional. *Control, Optimisation, and Calculus of Variations*, to appear. Available online at <http://www.math.umn.edu/%7Easantosa/fs.html>.

- [46] F. Santosa. A level-set approach for inverse problems involving obstacles. *ESAIM Contrôle Optim. Calc. Var.*, 1:17–33 (electronic), 1995/96.
- [47] J. A. Sethian. Fast marching methods. *SIAM Rev.*, 41(2):199–235 (electronic), 1999.
- [48] J. A. Sethian. *Level set methods and fast marching methods*, volume 3 of *Cambridge Monographs on Applied and Computational Mathematics*. Cambridge University Press, Cambridge, second edition, 1999. Evolving interfaces in computational geometry, fluid mechanics, computer vision, and materials science.
- [49] J. A. Sethian and J. Strain. Crystal growth and dendritic solidification. *J. Comput. Phys.*, 98(2):231–253, 1992.
- [50] B. Song and T.F. Chan. Fast algorithm for level set segmentation. *UCLA CAM report 02-68*, 2002.
- [51] X.-C. Tai and T. Karkainen. Identification of a nonlinear parameter in a parabolic equation from a linear equation. *Comp. Appl. Mat.*, 14:157–184, 1995.
- [52] Xue-Cheng Tai and Pekka Neittaanmaki. Error estimates for numerical identification of distributed parameters. *J. Comp. Math.*, Supplementary issue:66–78, 1992.
- [53] Xue-Cheng Tai and Pekka Neittaanmaki. Pointwise error estimates for distributed parameter identification. In D. Bainov, editor, *Proceedings of the seventh international colloquium on differential equations*, pages 455–468, The Netherlands, 1997. International Science Publishers.
- [54] Y.R. Tsai, L.T. Cheng, S. Osher, and H.K. Zhao. Fast sweeping algorithms for a class of hamilton-jacobi equations. *SIAM J. Numer. Anal.*, to appear.
- [55] Luminita A. Vese and Tony F. Chan. A new multiphase level set framework for image segmentation via the Mumford and Shah model. *International Journal of Computer Vision*, 50:271–293, 2002.
- [56] H. K. Zhao. Fast sweeping method for eikonal equations i. *SIAM J. Numer. Anal.*, to appear.
- [57] Hong-Kai Zhao, T. Chan, B. Merriman, and S. Osher. A variational level set approach to multiphase motion. *J. Comput. Phys.*, 127(1):179–195, 1996.

Department of Mathematics, University of Bergen, Johannes Brunsgate 12, N-5009 Bergen, Norway

*E-mail:* tai@mi.uib.no

*URL:* <http://www.mi.uib.no/%7Etai>

Department of Mathematics, University of California, Los Angeles, 405 Hilgard Avenue, Los Angeles, CA 90095-1555. USA

*E-mail:* TonyC@college.ucla.edu

*URL:* <http://www.math.ucla.edu/%7Echan>